Dalton Transactions

ROYAL SOCIETY OF CHEMISTRY

PAPER

Check for updates

Cite this: *Dalton Trans.*, 2022, **51**, 7539

Anticancer and biological properties of new axially disubstituted silicon phthalocyanines†

Nazli Farajzadeh, [a] Nilgün Güler Kuşçulu,[b] H. Yasemin Yenilmez,[a] Dilek Bahar[c] and Zehra Altuntaş Bayır *[a]

Received 4th April 2022,
Accepted 18th April 2022

DOI: 10.1039/d2dt01033j

rsc.li/dalton

This study reports the synthesis of three novel axially disubstituted silicon phthalocyanines (**1–3-Si**) and their quaternized phthalocyanines (**1–3-QSi**). The resulting compounds were characterized by applying spectroscopic techniques including ^{1}H NMR, FT-IR, UV–vis, and mass spectroscopy. The biological properties of compounds **1–3-QSi**, including DNA cleavage activities, DNA binding modes, and topoisomerase enzyme inhibition activities, were investigated using agarose gel electrophoresis. pBR322 plasmid DNA, CT-DNA, and AL-DNA (isolated from apricot leaf) were used for DNA studies. All the quaternized compounds exhibited acceptable DNA cleavage activities. Human topoisomerase I and *E. coli* topoisomerase enzymes were used for the topoisomerase I inhibition studies. All the quaternized complexes inhibited topoisomerase I activity. Moreover, these compounds were screened for cytotoxic and apoptotic effects against a human colon cancer cell line (DLD-1) by performing MTT and Annexin V assays. They exhibited toxicity and apoptotic effect on the DLD-1 cell line. The findings reveal that the compounds can be utilized for cancer therapy after further investigations.

Introduction

Phthalocyanines as porphyrin analogs include a planar aromatic 18π-electron ring (Pc ring). This structure results in high electron transfers that in turn make phthalocyanines suitable materials for a wide range of high-tech applications.[1–4] However, aggregation of phthalocyanines significantly decreases their solubility in organic and aqueous media. The low solubility of phthalocyanines limits their utility in different applications that require soluble materials. An increase in the distance between the Pc rings of phthalocyanines can be followed by a decrease in π-stacking interactions between these structures, leading to less aggregation and more solubility. For this purpose, the periphery of the Pc ring is substituted by long and/or bulky substituents such as alkoxy, alkylthioxy, and phenoxy groups. Moreover, the insertion of metal ions into the Pc cavity can improve solubility. Also, some of the metal cations that have higher coordination numbers (more than 2) include axial ligands inserted into the ring center.[5–15] The presence of axial ligands in the structure of phthalocyanines intensively reduces the π–π interactions and results in much more soluble phthalocyanines.[1–4] Depending on a special function, different ligands can be placed in axial positions. Generally, axial substitution of a bulky group decreases aggregation and increases solubility more than α- and β-substitution of the same group in the Pc ring.[16,17] The introduction of substituents on non-peripheral (α-) and peripheral (β-) positions of the Pc ring leads to a significant change in the absorption and emission spectra in comparison with alteration of the axial ligand.[18–21]

Among the diverse metal phthalocyanines, silicon phthalocyanines have attracted more attention due to the extraordinary hexacoordinated silicon(IV) and the chemical stability of the Si–N bonds.[16] In addition, the existence of a bond between silicon and oxo-, thio-, and C-connected ligands on axial positions shifts the electronic absorption spectra of silicon phthalocyanines to longer wavelengths. Due to the red shifts, silicon phthalocyanines become efficient materials for near-infrared and infrared applications such as photodynamic therapy, photocatalytic systems, electrochromic devices, photovoltaic cells, and medicinal biology.[22–24] Additionally, the Si–N bonds result in excellent acidic and basic stability of silicon phthalocyanines.[16]

DNA is a life-basis biopolymer that contains polynucleotides and plays an important role in metabolic activities in living systems, protein synthesis, and genetic diseases. Thus it has become an essential molecule studied in the diagnosis

[a]*Department of Chemistry, Istanbul Technical University, TR-34469 Istanbul, Turkey. E-mail: bayir@itu.edu.tr*
[b]*Department of Chemistry Technology, Mustafa Çıkrıkçıoğlu Vocational School, Kayseri University, TR-38280 Kayseri, Turkey*
[c]*Genome & Stem Cell Center (GENKOK), Erciyes University, TR-38280 Kayseri, Turkey*

† Electronic supplementary information (ESI) available. See DOI: **https://doi.org/10.1039/d2dt01033j**

and treatment of many diseases, especially cancer, that may occur in living metabolism.[25–27]

Cancer can also be defined as a term that covers a large number of different uncontrolled-growth tumors. Indeed, a pathogenic condition is not just uncontrolled cell proliferation and growth. It can also be expressed by tumor cell migration, invasion, and spread to other organs and tissues under special conditions. Different physical factors and environments can transform normal cells into cancerous cells by altering the normal function of a wide range of regulatory, apoptotic, and signal transduction pathways.[27,28] According to the World Health Organization report, approximately 16.6 percent of deaths result from cancer. According to the American Cancer Society report, 21.6 million new cancer cases will be detected worldwide in 2030, which will result in 13 million deaths.[29] Albeit surgery, chemotherapy, and radiotherapy are known to be effective cancer therapies, cancerous cells can exhibit resistance to the drugs. Also, the applied drugs can be toxic in some cases. Therefore, new treatment drugs and approaches are being developed to overcome these problems. As phthalocyanines exhibit efficient anticancer features, scientists have been interested in these new subtypes in recent years.[30–39] In addition, it is essential to know and understand the chemical structure of genomic DNA, which is located in the cell nucleus and has many crucial functions in the living system, to provide new drugs, because this will help us to understand the binding mechanism of many molecules, such as phthalocyanines, that will interfere with DNA and change its function in the desired direction. In the DNA the helix structure, phosphate skeleton, double helix, and sugar structure are the same in all living species, while the length of the DNA helix, the number of base pairs, the distance between the two helixes (width), the size of the major and minor grooves formed between the helixes, the number, and type of base pairs are different. Accordingly, there are three different DNA conformations, A, B, and Z. The B and Z DNA forms are mostly found in existing living species.[40] Cancer cells proliferate uncontrollably. This means that DNA replication increases. In this case, chemical structures are needed to slow down and prevent replication.[28] In replication, topoisomerase enzymes help to open the ds (DNA). However, the temperature and pH of the environment affect the formation of ss (DNA) from ds (DNA). Here, a reversible reaction takes place. When the replication is completed, the ss (DNA) chain is closed and ds (DNA) formation occurs. In this reaction, the numerical excess in the G–C base pair content of the helix increases the stability of the DNA structure, as well as environmental factors. The percentage G–C base pair content differs in living species.[41] However, plant and animal DNA models differ in the size of major and minor grooves and chain lengths.[42] Pesticides are important compounds that combat different pests. An appropriate pesticide controls, prevents, or kills target pests without having any toxic effect on the protected products.[43] As herbal products are extensively consumed all over the world, healthy herbal cultivation is a vital issue.[44,45] Generally, genomic DNA of apricot leaf (AL-DNA) is used as a genomic plant DNA model for the study of genetic diseases in plants.[46] In this study, the interaction between phthalocyanines and AL-DNA extracted from an apricot leaf has been studied for the first time to measure the potential utility of phthalocyanines as herbicides in the farming industry.

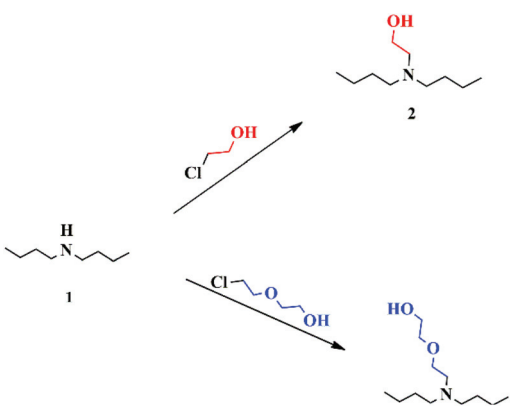
Topoisomerase I and II are topoisomerase enzymes that cut and reassemble DNA strands. These enzymes can change the topological state during cell proliferation (replication, transcription, and recombination). As a result, these enzymes can play vital roles in the treatment of cancers, since they expand in the abnormal cells much more than in healthy cells.[47,48] Irinotecan, doxorubicin, and camptothecin are some efficient topoisomerase inhibition agents that are utilized clinically in cancer cures. However, these inhibitors have some side effects, including fever, cardiotoxicity, tremor, and immune systemic depression. Additionally, they have high drug resistance and chemical instability as well as poor solubility in water.[49,50] Hence researchers have been encouraged to investigate new topoisomerase inhibitors that can overcome these problems.

This study presents a series of new axially substituted silicon phthalocyanines bearing amines with different lengths. Moreover, the effect of the length of the ligands on the biological properties of silicon phthalocyanines was studied by applying molecular biological tests. In this study, the interaction between quaternized phthalocyanines (**1–3-QSi**) and a number of different DNA molecules (CT-DNA, supercoiled pBR322DNA, and genomic AL-DNA) was investigated by performing absorption spectroscopy and gel electrophoresis assays. In addition, the topoisomerase I enzyme inhibition activity and anticancer drug potential of the quaternized phthalocyanines were examined. Moreover, the compounds' cytotoxic effects were tested using 3-(4,5-dimethylthiazol-2-yl)-2,5-diphenyltetrazolium bromide (MTT) and Annexin V assays.

Results and discussion

Synthesis and characterization

The synthetic procedures for compounds **2** and **3** are depicted in Scheme 1. Compounds **2** and **3** resulted from the combi-



Scheme 1 The synthetic pathway for compounds **2 and 3**. NaOH, EtOH, 70 °C.

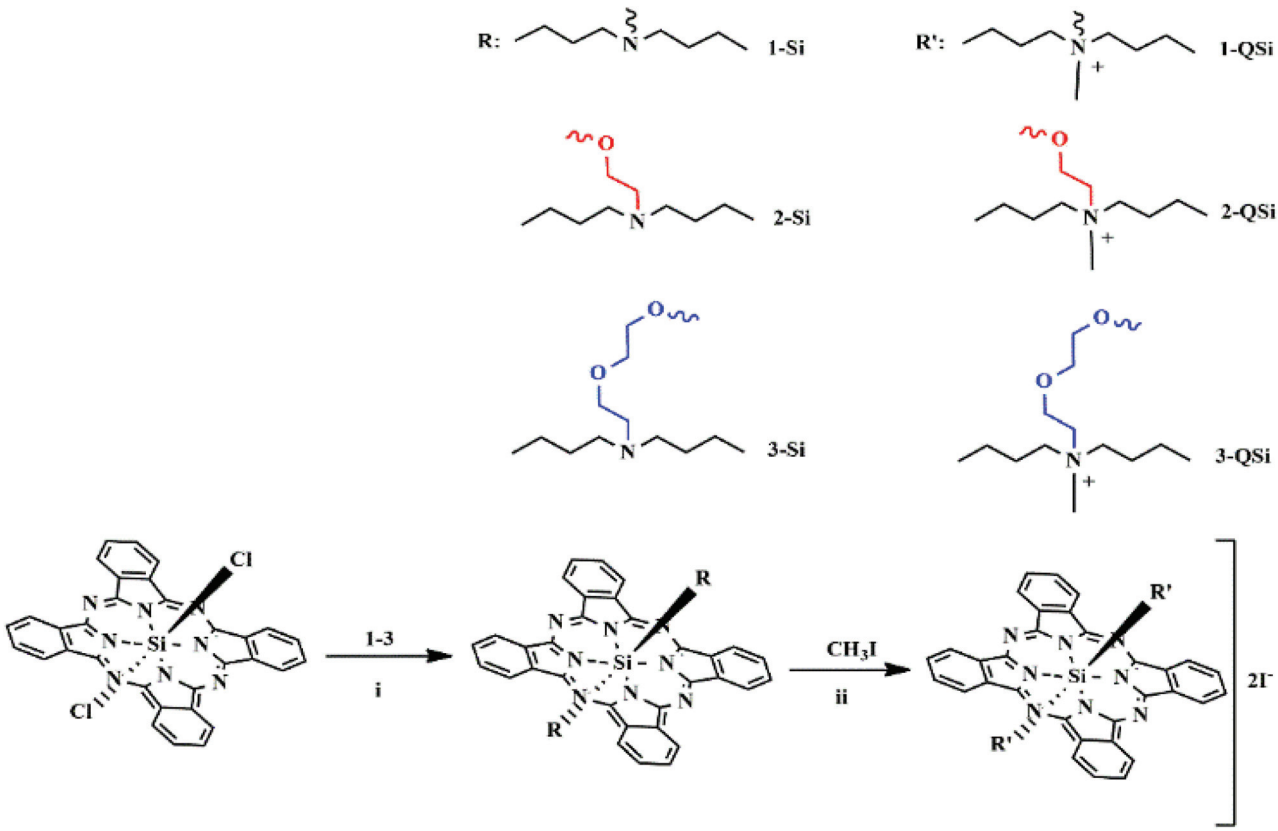
This journal is © The Royal Society of Chemistry 2022

nation of compound **1** and 2-chloroethanol or 2-(2-chloroethoxy) ethanol in the presence of sodium hydroxide for base catalysis in ethanol. The pure product was eluted from silica gel column chromatography with methanol. The resultant compounds were characterized by performing ^{1}H NMR, ^{13}C NMR, and FT-IR spectroscopies. The obtained results confirmed the synthesis of the target compounds. Based on the FT-IR data, CH_2–OH vibration bands were observed at around 3400 cm^{-1}. In the ^{1}H NMR spectra of compounds **2** and **3**, the protons of OH appeared at 5.37 and 5.75 ppm, respectively.

Scheme 2 portrays the synthetic routes for silicon phthalocyanines (**1–3-Si** and **1–3-QSi**). Silicon phthalocyanine dichloride and the related ligand (compounds **1–3**) participated in a nucleophilic substitution reaction in the presence of sodium hydride as a base and silicon phthalocyanines (**1–3-Si**) were synthesized. These complexes were purified by performing silica-gel column chromatography with *n*-hexane : THF (1 : 1) as the eluent. The quaternized silicon phthalocyanines (**1–3-QSi**) were prepared by the dissolution of complexes **1–3** and iodomethane in chloroform at room temperature for two days. The solid was filtered off and washed several times with chloroform. All the newly synthesized compounds were characterized using different spectroscopic techniques, such as ^{1}H NMR, FT-IR, and UV–vis spectroscopies. All the data were in agreement with the proposed structures. In the FT-IR spectra of all the resultant compounds, the CH_2–OH vibration bands disappeared with the formation of Si–O–CH_2 bonds. In the ^{1}H NMR spectra of compounds **1–3-Si** and **1–3-QSi**, aromatic protons were observed between 9.09 and 7.35 ppm as broadening singlets or multiplets. Each of these bands was integrated into eight protons of peripheral aromatic protons or eight protons of non-peripheral ones. Except for compounds **1-Si** and **1-QSi**, the aliphatic protons of the chain connected to silicon shifted to the strong magnetic fields owing to the magnetic anisotropy of phthalocyanine rings. Therefore, the related bands appeared between 0.08 and −2.61. In the mass spectra of compounds **1–3-QSi**, molecular ion peaks were obtained at 370.790 $[M + Na + 3H]^{3+}$ and 1098.322 $[M + H_2O]^{+}$ for compound **1-QSi**, 801.787 $[M - 2C_4H_9 - 2I]^{+}$, 1019.596 $[M - C_4H_9 - I + 2H_2O]^{+}$, 1169.825 $[M]^{+}$, 1226.733 $[M + Na + 2H_2O - 2H]^{+}$ and 1284.636 $[M + 2Na + 3H_2O - 2H]^{+}$ for compound **2-QSi**, and 557.856 $[M - CH_3 - I]^{2+}$ and 1669.429 $[M + 2DHB + 3Na + 2H_2O]^{+}$ for compound **3-QSi**.

UV–vis spectra

The unique properties of phthalocyanines arise from their two-dimensional 18π-electron structure, which results in high electron-transferring abilities. Therefore, any change in their electronic transfers is followed by an electronic absorption alteration that in turn can be studied using the UV–vis spectra. Hence, examination of these spectra is useful to manage the electronic and optical features of phthalocyanines. The elec-



Scheme 2 The synthetic pathway for compounds **1–3-Si** and **1–3QSi**. (i) NaH, toluene, 130 °C; (ii) chloroform, room temperature.

tronic absorption spectra of two strong bands in the ultraviolet region (300–400 nm, B-band) and visible region (around 700 nm, Q-band) were examined. The Q-band corresponds to π–π* transitions from HOMO to LUMO whereas the B-band is assigned to π–π* transitions from deeper π-orbitals to LUMO. In addition, the temperature, the substituent (type and position), and the solvent nature are essential parameters that can shift these bands, especially the Q-band.[1–4]

In this study, the UV–vis spectra of compounds **1–3-Si** and **1–3-QSi** were studied in DMSO at room temperature (Fig. 1). Since DMSO could not coordinate axially with the metal ion, the existence of aggregation between the monomer phthalocyanines is non-negligible.[51–53] In the literature, there are some silicon phthalocyanines that exhibit similar UV–vis properties.[54–56] As shown in Fig. 1, the electronic absorption of macromolecules **2-Si** and **3-Si** was blue-shifted in comparison with that of compound **1-Si**. However, the quaternized silicon phthalocyanines were similar to the related silicon phthalocyanines.[35] In addition, the biological measurements obtained for the new quaternized silicon phthalocyanines are compatible with the literature, despite the presence of the aggregated species in DMSO.[54–56]

DNA cleavage activity

DNA is a vital molecule for all living cells and it can be mutated, and in turn, threaten the living organisms. As metal complexes have attracted intensive attention owing to their excellent biological properties, the interactions between DNA and metal complexes have been explored in recent years.[35,57] Therefore, the DNA cleavage activity of materials such as metallophthalocyanines has been studied for the design of new drugs, particularly anticancer and antimicrobial ones.[13,31,32] In this study, the pBR322 plasmid DNA cleavage activity of compounds **1–3-QSi** was examined by applying gel electrophoresis without irradiation. All the results are shown in Fig. 2. As demonstrated, compounds **1–3-QSi** cleaved the supercoiled form (SC, form I) into the nicked circular form (NC, form II) in the dark (lanes 2–10). Although they exhibited

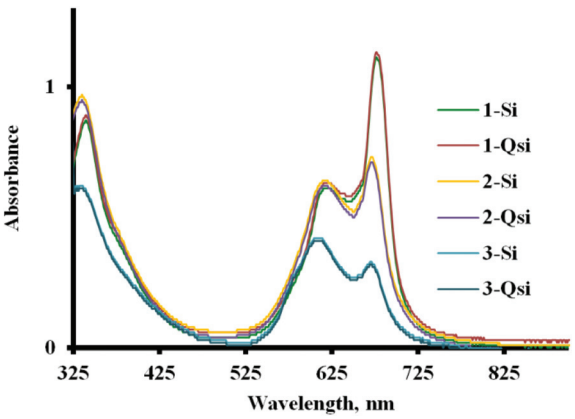


Fig. 1 The UV–vis spectra of compounds **1–3-Si** and **1–3-QSi** in DMSO at room temperature (conc.: 6 μM).

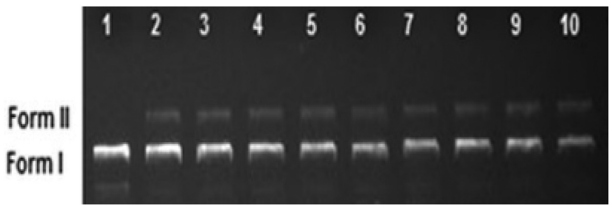


Fig. 2 DNA cleavage activities of compounds **1–3-QSi**. Lane 1, pBR 322DNA + 10 μL DMSO. Lane 2, pBR322DNA + 200 μg mL^{-1} of **1-QSi**. Lane 3, pBR 322DNA + 100 μg mL^{-1} of **1-QSi**. Lane 4, pBR 322DNA + 50 μg mL^{-1} of **1-QSi**. Lane 5, pBR 322DNA + 200 μg mL^{-1} of **2-QSi**. Lane 6, pBR 322DNA + 100 μg mL^{-1} of **2-QSi**. Lane 7, pBR 322DNA + 50 μg mL^{-1} of **2-QSi**. Lane 8, pBR 322DNA + 200 μg mL^{-1} of **3-QSi**. Lane 9, pBR 322DNA + 100 μg mL^{-1} of **3-QSi**. Lane 10, pBR 322DNA + 50 μg mL^{-1} of **3-QSi**.

DNA cleavage activities at all the studied concentrations, these interactions were not strong. Also, DMSO resulted in DNA breakage in a different direction (lane 1). The obtained results were compared with the literature. Baş *et al.* investigated the DNA cleavage activities of the new quaternized silicon phthalocyanine and naphthalocyanine bearing {[3-(4-acetylpiperazin-1-yl)propoxy]phenyl}methoxy groups with/without irradiation. The silicon complexes did not display any activity without irradiation.[35] Xiao *et al.* studied the DNA cleavage activity of fluorinated and non-fluorinated dendritic silicon(IV) phthalocyanines towards supercoiled plasmid DNA. The examined compounds did not display any cleavage activity without irradiation.[58] Compared with the literature, compounds **1–3-QSi** can be used as suitable materials in chemotherapy applications in addition to photodynamic therapy.

CT-DNA binding studies

The binding of the quaternized phthalocyanines (**1–3-QSi**) with CT-DNA was visualized using an agarose gel electrophoresis. All the samples included 50 μM of the target phthalocyanine. Different concentrations of CT-DNA ranging from 0.25 mg mL^{-1} to 2 mg mL^{-1} were added to the samples. The results are depicted in Fig. 3. As the ratio of CT-DNA/target compound increased, the intensity of CT-DNA was reduced. Although all the compounds interacted with CT-DNA through groove binding or intercalation, compounds **2-QSi** and **3-QSi** exhibi-

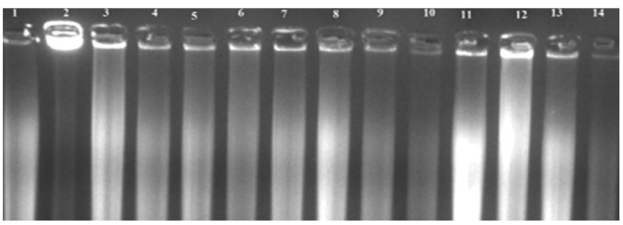


Fig. 3 Agarose gel electrophoresis of compounds **1–3-QSi**. Ingredients of lanes: lane 1, CT-DNA (2 mg mL^{-1}) in DDW; lane 2, CT-DNA (2 mg mL^{-1}) in buffer (pH = 7); lanes 3–6, CT-DNA (2–0.25 mg mL^{-1}) + buffer + compound **1-QSi** (50 μM); lanes 7–10, CT-DNA (2–0.25 mg mL^{-1}) + buffer + compound **2-QSi** (50 μM); lanes 11–14, CT-DNA (2–0.25 mg mL^{-1}) + buffer + compound **3-QSi** (50 μM).

This journal is © The Royal Society of Chemistry 2022

ted better DNA binding activities. There are similar studies in the literature. For instance, Baş *et al.* studied the interaction between CT-DNA and the new quaternized silicon phthalocyanine and naphthalocyanine bearing {[3-(4-acetylpiperazin-1-yl)propoxy]phenyl}methoxy groups. As the DNA concentration decreased, the interaction between the DNA and the studied macromolecules increased owing to complete neutralization of the negative charges of DNA by the tested compounds.[35]

Determination of the binding of compounds 1–3QSi to CT-DNA using UV–vis measurements

Generally, the binding mode of compounds with DNA molecules (intercalative or non-intercalative mode) is investigated by performing UV–vis spectroscopy. For intercalative interactions, an increase in DNA concentration leads to a bathochromic shift of the UV–vis spectra along with a decrease in the absorbance intensity. However, non-intercalative interactions between compounds and DNA molecules result in a hypsochromic shift and an increase in absorbance intensity *via* the enhancement of DNA concentration. In this study, the UV–vis spectra of compounds **1–3-QSi** were obtained in the absence and presence of different concentrations of CT-DNA after incubation for 1 hour at 37 °C. The changes in the UV–vis spectra of compounds **1–3-QSi** were studied at 677, 670, and 669 nm, respectively. All the data are listed in Table 1. An increase in the DNA concentration was followed by a decrease in the Q-band intensity of the UV–vis spectra of compounds **1–3-QSi** along with a slight red shift. The results indicate that CT-DNA intercalated or interacted electrostatically with the studied phthalocyanines. According to the K_b values, compound **2-QSi** exhibited the highest CT-DNA binding activity whereas compound **1-QSi** displayed the lowest activity. Some studies in the literature report similar results. Barut *et al.* investigated the binding mechanism of water-soluble silicon phthalocyanines bearing morpholinophenoxy groups on axial positions and CT-DNA. As the DNA concentration increased, the Q-band intensity decreased and shifted to the red region. These results proved that the phthalocyanines bound to CT-DNA through the intercalation mode.[32] Also, Baş *et al.* studied the binding mode between CT-DNA and the new axially disubstituted quaternized silicon phthalocyanine bearing {[3-(4-acetylpiperazin-1-yl)propoxy]phenyl}methoxy groups. The compound exhibited the same behavior.[35] Therefore, the obtained results for the CT-DNA binding studies of compounds **1–3-QSi** were compatible with the literature.

Table 1 CT-DNA binding data for compounds **1–3-QSi**

Compound	Wavelength (nm)	Change in absorbance	Red shift (nm)	K_b (M^{-1})
1-QSi	677	Hypochromism	2	1.6×10^4
2-QSi	670	Hypochromism	1	9.0×10^4
3-QSi	669	Hypochromism	1	5.0×10^4

AL-DNA (isolated from apricot leaf) binding

The binding of the quaternized phthalocyanines (**1–3-QSi**) with AL-DNA was studied by performing agarose gel electrophoresis. In this study, the samples contained the constant amount of the target phthalocyanine (50 μM) and various concentrations of AL-DNA (0.50–2 mg mL^{-1}). The results are shown in Fig. 4. The first three lanes are correlated to the samples including only AL-DNA. As shown in Fig. 4, 200 μM of compound **2-QSi** or **3-QSi** caused an increase in DNA flashing intensity, especially in lanes 7 and 10. As a result, compounds **2-QSi** and **3-QSi** can intercalate like ethidium bromide. However, the DNA band disappeared in lanes 6, 8, and 9 as the concentration of AL-DNA decreased. The disappearance of the DNA lanes confirmed that the neutralization occurred by the interaction of the negatively charged phosphate backbone of AL-DNA with the positively charged-N^+ centre of phthalocyanines. Due to the loss of interaction between compound **3-QSi** and AL-DNA, its potential as a suitable pesticide can be investigated in further studies.

Topoisomerase inhibition

The DNA relaxation assay is a well-known approach to examine the topoisomerase inhibition properties of materials. This method is carried out by applying agarose gel electrophoresis.[59–61] In this study, the human and *E. coli* topoisomerase I enzyme inhibition activities of compounds **1–3-QSi** were examined. The obtained agarose gel electrophoresis images are demonstrated in Fig. 5 and 6.

Irinotecan was used as a positive control to investigate the inhibition activity of compounds **1–3-QSi** in the human topoisomerase I enzyme (Fig. 5).[35,62,63] The test method extensively described in ref. 63 was applied with some modifications. Lane 3 was used as a negative control. As shown, Topo I led to the separation of the pBR322DNA supercoiled structure, while the buffer solution exhibited a different behaviour (lane 4). In addition, no conversion from Form I to Form II or Form III was observed in the other lanes. In comparison with the control, compounds **1–3-QSi** inhibited DNA supercoiled segregation and thereby displayed effective human topoisomerase I enzyme inhibition (lanes 14–16). As shown in Fig. 6, the Topo I enzyme was inactive in the absence of the buffer (lane 3). However, Topo-I resulted in the relaxation of the DNA super-

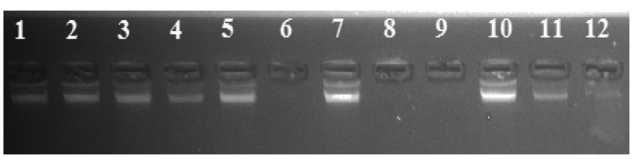


Fig. 4 Agarose gel electrophoresis of compounds **1–3-QSi**. Ingredients of lanes: lane 1, AL-DNA (2 mg mL^{-1}) in DDW; lane 2, AL-DNA (2 mg mL^{-1}) in buffer (pH = 7); lane 3, AL-DNA (2 mg mL^{-1}) in DMSO; lanes 4–6, AL-DNA (2–0.5 mg mL^{-1}) + buffer + compound **1-QSi** (50 μM); lanes 7–9, AL-DNA (2–0.5 mg mL^{-1}) + buffer + compound **2-QSi** (50 μM); lanes 10–12, AL-DNA (2–0.5 mg mL^{-1}) + buffer + compound **3-QSi** (50 μM).

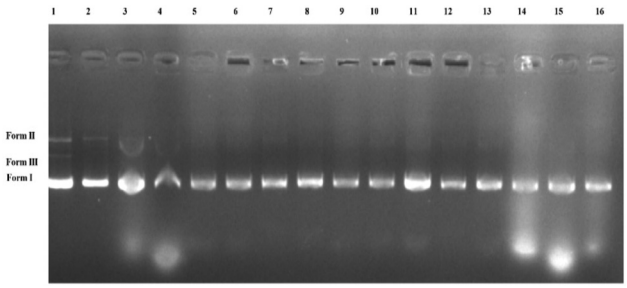


Fig. 5 The inhibitory effects against human topoisomerase I of compounds **1–3-QSi**. Lane 1, pBR322 in DDW; lane 2, pBR322 in buffer (TGS) and water; lane 3, pBR322 + 1 Unit Topo I; lane 4, pBR322 + 1 Unit Topo I + buffer (TGS) + DDW; lanes 5–7, pBR322 + 1 Unit Topo I + buffer (TGS) + compound **1-QSi** (200, 100, 50 μM) + DDW; lanes 8–10, pBR322 + 1 Unit Topo I + buffer (TGS) + compound **2-QSi** (200, 100, 50 μM) + DDW; lanes 11–13, pBR322 + 1 Unit Topo I + buffer (TGS) + compound **3-QSi** (200, 100, 50 μM) + DDW; lanes 14–16, pBR322 + 1 Unit Topo I + buffer (TGS) + irinotecan (200, 100, 50 μM) + DDW.

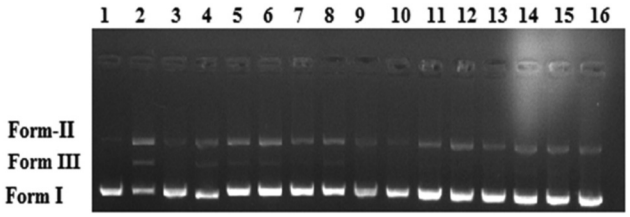


Fig. 6 The inhibitory effects against *E. coli* topoisomerase I of compounds **1–3-QSi**. Lane 1, pBR322 in DDW; lane 2, pBR322 in buffer and DDW; lane 3, pBR322 + Topo I in DDW; lane 4, pBR322 + 1 Unit Topo I + buffer + DDW; lanes 5–7, pBR322 + 1 Unit Topo I + buffer + compound **1-QSi** (200, 100, 50 μM) + DDW; lanes 8–10, pBR322 + 1 Unit Topo I + buffer + compound **2-QSi** (200, 100, 50 μM) + DDW; lanes 11–13, pBR322 + 1 Unit Topo I + buffer + compound **3-QSi** (200, 100, 50 μM) + DDW; lanes 14–16, pBR322 + 1 Unit Topo I + buffer + irinotecan (200, 100, 50 μM) + DDW.

coiled helix in the presence of the buffer (lane 4). Also, the DNA helix was opened twice and converted from Form I to Form II and Form III. The samples including different concentrations of compounds **1–3-QSi** were prepared by dilution with DMSO (lanes 5–13). Irinotecan was used as a positive control (lanes 14–16). Irinotecan prevented only the formation of Form III that resulted from *E. coli* topoisomerase I activation. Probably, compounds **2-QSi** and **3-QSi** acted as positive agents and prevented Form III formation. Therefore, these compounds can inhibit the activation of the *E. coli* topoisomerase I enzyme. However, compound **1-QSi** could not prevent the formation of Form II and Form III from Form I in the DNA helix and three forms were formed in lanes 5–7. As a result, compound **1-QSi** cannot be used as an *E. coli* Topo I enzyme inhibitor. There are similar studies in the literature. Barut *et al.* reported the human topoisomerase I inhibition activity of water-soluble zinc(II) phthalocyanine bearing 3-morpholinophenoxy substituents. The zinc(II) phthalocyanine inhibited the topoisomerase I enzyme in a concentration-dependent manner.[64] Demirtaş studied the *E. coli* topoisomerase I inhibition features of peripherally tetra-substituted zinc phthalocyanine bearing 1-phenoxypropan-2-yloxy groups. The zinc complex displayed *E. coli* topoisomerase I inhibition activity.[65] Shuai *et al.* prepared a series of new cationic metal-free, copper, zinc, and nickel porphyrins and phthalocyanines bearing various amino alcohols and investigated their DNA topoisomerase I inhibition features. The cationic meso-substituted porphyrins and cationic phthalocyanine inhibited the interaction between Topo I and DNA.[66] Additionally, Keleş *et al.* studied the topoisomerase I inhibition activity of axially [3,5-bis3-pyridin-4-ylpropoxyphenyl]methoxy group-substituted silicon(IV) phthalocyanine and naphthalocyanine.[62] They exhibited inhibition effects against topoisomerase I. Compared with the literature, the newly synthesized compounds (**1–3-QSi**) displayed relatively high topoisomerase I inhibition activities and can be used in medicine after further investigation.

Cell culture

Cell culture is a commercial tool that is mostly utilized in cellular and molecular biology. It is a suitable approach to study mutagenesis and carcinogenesis, the effect of drugs and toxic compounds on the cells, and the normal physiology and biochemistry of cells. It is also well known as a consistent and reproducible application for a batch of clonal cells.

Generally, the shape, size, and surface of the anticancer drugs are important parameters that affect tissue penetration and drug delivery.[67] There are various aminated materials that have been used for cancerous cells since these positively charged compounds accumulate in the outer layer of cancer cells much more than negatively charged or neutral compounds.[68–71] In this study, the DLD-1 cell line was cultured in normal culture conditions without any contamination. The control and DMSO control maintained the original morphology of the tested cells during cell culture. As expected, the morphology of the cells incubated with compounds **1–3-QSi** abnormally changed and their structures shrank. The results are demonstrated in Fig. 7.

MTT assay

The MTT assay is an appropriate method to evaluate cellular metabolic activity. This method acts as an indicator to measure cell viability, proliferation, and cytotoxicity.[72–74] In this study, the phototoxic effect of compounds **1–3-QSi** on the DLD-1 cell lane was studied using an MTT cell proliferation assay as an *in vitro* cytotoxic method. The IC_{50} values are listed in Table 2. The obtained cytotoxic and phototoxic results are depicted in Fig. 8. The cell proliferation decreased as the concentration of compounds **1–3-QSi** increased. However, a statistically significant change was not observed by applying the white lamp irradiation group ($P < 0.05$). The IC_{50} values confirmed that compounds **1–3-QSi** can inhibit the proliferation of DLD-1 cells. Their cytotoxicity on the DLD-1 cell line decreased in the following order: **3-QSi** > **1-QSi** ≥ **2-QSi**. Some similar studies have been presented in the literature. Zheng

 This journal is © The Royal Society of Chemistry 2022

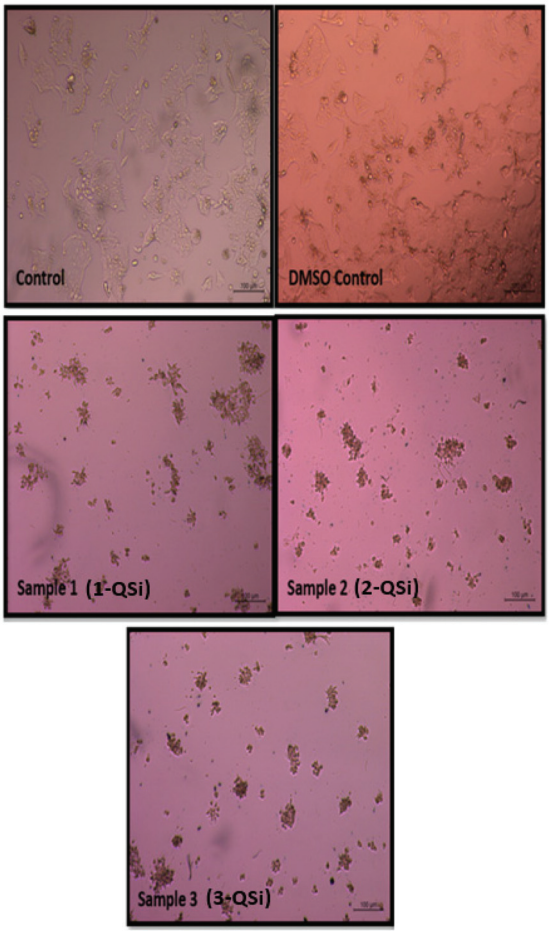


Fig. 7 The microphotographs of the DLD-1 cells. Cell morphologic character with 100 μM of each compound (**1–3-QSi**) and control groups, for 24 hours, under inverted microscopy ×10.

Table 2 IC_{50} values of compounds **1–3-QSi** on DLD-1 cell lane

	IC_{50} values (μM)	
Compounds	Dark irradiation	White irradiation
1-QSi	13.33	11.11
2-QSi	14.16	16.46
3-QSi	10.61	11.08
Cisplatin	80.6	80.5

et al. examined the photodynamic activities of symmetric or unsymmetric silicon(IV) phthalocyanines bearing a cyclic Arg-Gly-Asp (cRGD) group on axial positions against HT-29 human colon carcinoma cells and MCF-7 human breast adenocarcinoma cells. The IC_{50} values were obtained between 0.2 and 100 μM for the silicon phthalocyanines.[75] Aru *et al.* investigated the anticancer efficacy of a silicon phthalocyanine axially substituted with 3-hydroxypyridin-2-thione cells on breast cancer cell lines and a healthy human endothelial cell line.[76] The IC_{50} values were determined between 9.2 and 42 μM. In comparison with the literature, compounds **1–3-QSi**

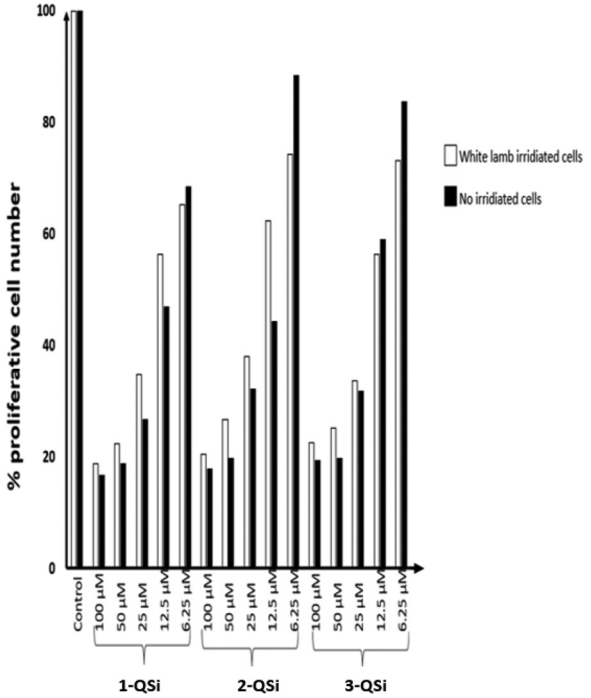


Fig. 8 Cell proliferation (%) at different concentrations of compounds **1–3-QSi** with/without white lamp irradiation.

can be utilized as efficient anticancer drugs in photodynamic applications as well as chemotherapy.

Apoptosis assay

Apoptosis is defined as programmed cell death, playing an important role in development, aging, and disease. MTT-like viability tests measure the cytotoxicity effect of compounds on cells, whereas the apoptotic effect is a result of the cell checkpoint process to deport unwanted damaged cells.[77–79] In this study, the *in vitro* apoptotic effect of compounds **1–3-QSi** on the DLD-1 cell line was investigated by performing Annexin V assays. The live cells, early and late apoptosis, and cell death (total apoptotic) were analyzed in the DLD-1 cells using the Annexin V assay kit. The obtained results are shown in Fig. 9. Since the application of the white lamp irradiation did not make a significant change in the MTT test, the apoptosis studies were carried out without white lamp irradiation and only the IC_{50} values were determined to analyze the apoptotic effects of compounds **1–3-QSi**. Compound **2-QSi** led to the highest cell apoptosis despite its statistically insignificant effect. Although compounds **1-QSi** and **3-QSi** did not cause higher numbers of apoptotic cells in comparison with the live cells, these compounds induced apoptosis to a statistically significant extent ($P = 0.05$) compared with compound **1-QSi** and control group apoptotic cells. There are similar studies in the literature. Barge *et al.* synthesized a number of silicon phthalocyanines (SiPc) bearing bulky axial substituents that exhibited high apoptotic effects on M3Dau cells.[80] Rodriguez *et al.* synthesized a series of symmetric and unsymmetric axially di-

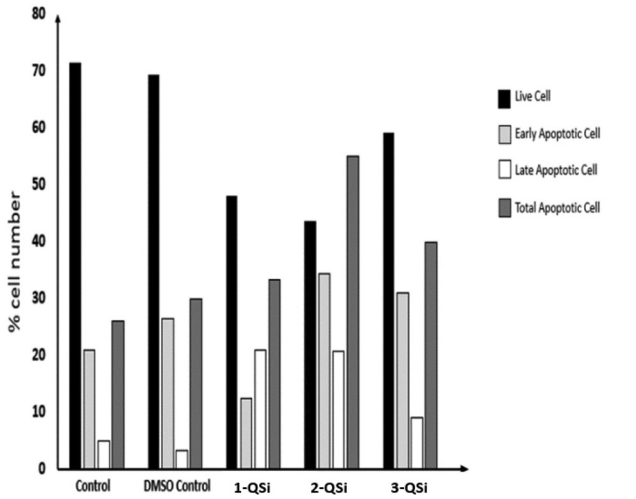


Fig. 9 Percentage of the DLD-1 cells apoptosis and live cells in the absence/presence of compounds **1–3-QSi**.

substituted silicon phthalocyanines bearing various amine and alkyl groups and examined their apoptotic properties. Most of the compounds displayed acceptable apoptotic behaviours.[81] In comparison with the literature, compatible apoptotic features were obtained for compounds **1–3-QSi**.

Experimental

Materials and equipment

All the biological and chemical materials were of reagent-grade quality and were obtained from commercial suppliers. Silicon (IV) phthalocyanine dichloride was purchased from Merck Company. Agarose (ısolab), dimethylsulfoxide (DMSO), double-distilled water (DDW), bromophenol blue, calf thymus deoxyribonucleic acid (CT-DNA), ethylenediaminetetraacetate (EDTA), sodium dodecyl sulfate (SDS), trisma-base (Tris), glycerol, loading dye, ethidium bromide (EtBr), irinotecan, doxorubicin, and silicon(IV) phthalocyanine dichloride were purchased from Sigma Aldrich Company. Supercoiled pBR322 plasmid DNA was obtained from Thermo Scientific. Human and *E. coli* topoisomerase I kits were purchased from Topogen. Apricot leaf was obtained from the Malatya region.

DNA isolation from apricot leaf

A quick, simple, and reliable method for the extraction of DNA from apricot leaves has been developed. This method, based on that of Doyle and Doyle (1990), is a CTBA-based extraction procedure modified by the use of NaCl to remove polysaccharides and PVP to eliminate polyphenols during DNA purification.[82]

Synthesis and characterization

General synthetic procedure for compounds 2 and 3. Compound **1** (500 mg, 3.87 mmol), 2-chloroethanol (311.48 mg, 3.87 mmol) or 2-(2-chloroethoxy)ethanol (481.91 mg, 3.87 mmol), and sodium hydroxide (618.94 mg, 15.47 mmol) were refluxed in ethanol (10 mL) for 48 hours under an inert atmosphere. The solid was filtered off and washed several times with ethanol. The pure product was obtained using column chromatography on silica gel with methanol as the eluent.

2-(Dibutylamino)ethanol (2). Yield 400 mg (59.66%). FT-IR ν (cm^{-1}): 3452 (OH), 2956–2920 (C–H aliphatic), 1120 (C–N). ^{1}H NMR (500 MHz; DMSO-d_6): δ (ppm) 5.37 (s, 1H, OH), 3.78 (bs, 2H, C**H$_2$**OH), 3.61–3.58 (m, 4H, 2 N–C**H$_2$**–CH_2–CH_2–CH_3), 2.53–2.50 (m, 2H, N–C**H$_2$**–CH_2–OH), 1.77–1.74 (m, 4H, 2 N–CH_2–C**H$_2$**–CH_2–CH_3), 1.30–1.23 (m, 4H, N–CH_2–CH_2–C**H$_2$**–CH_3), 0.93–0.90 (t, 6H, 2 CH_3). ^{13}C NMR (500 MHz; DMSO-d_6): δ (ppm) 60.14, 59.38, 57.80, 32.33, 22.76, 12.13.

2-(2-(Dibutylamino)ethoxy)ethanol (3). Yield 480 mg (57.04%). FT-IR ν (cm^{-1}): 3384 (OH), 2964–2928 (C–H aliphatic), 1379–1120 (C–N), 1090 (C–O–C). ^{1}H NMR (500 MHz; DMSO-d_6): δ (ppm) 5.75 (s, 1H, OH), 3.65–3.57 (m, 6H, C**H$_2$**–O–C**H$_2$**–C**H$_2$**–OH), 3.60–3.40 (m, 4H, 2 N–C**H$_2$**–CH_2–CH_2–CH_3), 2.54–2.51 (m, 2H, N–C**H$_2$**–CH_2–O), 1.77–1.74 (m, 4H, N–CH_2–C**H$_2$**–CH_2–CH_3), 1.24–1.21 (bs, 4H, N–CH_2–CH_2–C**H$_2$**–CH_3), 0.96–0.89 (t, 6H, 2 CH_3). ^{13}C NMR (500 MHz; DMSO-d_6): δ (ppm) 69.89, 69.85, 62.12, 57.95, 52.71, 34.08, 23.60, 13.50.

General synthetic procedure for compounds 1–3-Si. Silicon (IV) phthalocyanine dichloride (100 mg, 0.163 mmol) and the related ligand (compound **1** (42.27 mg, 0.327 mmol), compound **2** (56.68 mg, 0.327 mmol), or compound **3** (71.09 mg, 0.327 mmol)) were dissolved in toluene (3 mL). Then sodium hydride (31.39 g, 1.31 mmol) was added as the base to accelerate the reaction. The reaction mixture was stirred at 130 °C for 48 hours under a nitrogen atmosphere. The content was filtered off and washed several times with hot *n*-hexane and water. The crude product was purified by applying a column chromatographic technique on silica gel as the stationary phase and *n*-hexane–THF (1 : 1) as the mobile phase.

Compound 1-Si. Yield 30 mg (23%), mp >250 °C. FT-IR ν (cm^{-1}): 3063 (C–H aromatic), 2957–2926 (C–H aliphatic), 1334–1161 (C–N). ^{1}H NMR (500 MHz; DMSO-d_6): δ (ppm) 7.91–7.82 (m, 8H, Ar–H), 7.40–7.35 (m, 8H, Ar–H), 3.59 (bs, 8H, 4 N–C**H$_2$**–CH_2–CH_2–CH_3), 1.87–1.74 (m, 16H, 4 N–CH_2–C**H$_2$**–C**H$_2$**–CH_3), 1.22–1.13 (m, 12H, 4 N–CH_2–CH_2–CH_2–C**H$_3$**). UV–vis (DMSO): λ_{max} nm (log ε) 339 (5.16), 620 (5.00), 676 (5.26). Anal. calcd for $C_{48}H_{52}N_{10}Si$: C 72.33, H 6.58, N 17.57%, found: C 72.43, H 6.77, N 17.23%.

Compound 2-Si. Yield 58 mg (40%), mp >250 °C. FT-IR ν (cm^{-1}): 3015 (C–H aromatic), 2955–2853 (C–H aliphatic), 1377–1167 (C–N), 1074 (C–O–C). ^{1}H NMR (500 MHz; DMSO-d_6): δ (ppm) 9.09–8.91 (m, 8H, Ar–H), 8.46–8.41 (m, 8H, Ar–H), 3.62–3.55 (m, 8H, 4 N–C**H$_2$**–CH_2–CH_2–CH_3), 1.78–1.73 (m, 8H, 4 N–CH_2–C**H$_2$**–CH_2–CH_3), 1.39–1.32 (m, 8H, 4 N–CH_2–CH_2–C**H$_2$**–CH_3), 1.23–1.15 (m, 12H, 4 N–CH_2–CH_2–CH_2–C**H$_3$**), 0.06 (bs, 4H, 2 N–C**H$_2$**–CH_2–O–Si), −2.73 (bs, 4H, 2 N–CH_2–C**H$_2$**–O–Si). UV–vis (DMSO): λ_{max} nm (log ε) 335 (5.20), 617 (5.02), 670 (5.08). Anal. calcd for $C_{52}H_{60}N_{10}O_2Si$: C 70.56, H 6.83, N 15.82%, found: C 70.68, H 7.08, N 15.47%.

This journal is © The Royal Society of Chemistry 2022

Compound 3-Si. Yield 67 mg (42%), mp >250 °C. FT-IR ν (cm^{-1}): 3063 (C–H aromatic), 2922–2853 (C–H aliphatic), 1332–1162 (C–N), 1077 (C–O–C). ^{1}H NMR (500 MHz; DMSO-d_6): δ (ppm) 8.42 (bs, 8H, Ar–H), 7.72–7.60 (m, 8H, Ar–H), 3.18–3.15 (m, 8H, 4 N–C**H**$_2$–CH_2–CH_2–CH_3), 1.63–1.49 (m, 20H, 4 N–CH_2–C**H**$_2$–C**H**$_2$–CH_3, 2 N–C**H**$_2$–CH_2–O–CH_2–CH_2–O–Si), 0.86–0.82 (m, 12H, 4 N–CH_2–CH_2–CH_2–C**H**$_3$), 0.08–0.04 (m, 8H, 2 N–CH_2–C**H**$_2$–O–C**H**$_2$–CH_2–O–Si), −0.07 (bs, 4H, 2 N–CH_2–CH_2–O–CH_2–C**H**$_2$–O–Si). UV–vis (DMSO): λ_{max} nm ($\log \varepsilon$) 332 (5.01), 612 (4.84), 669 (4.74). Anal. calcd for $C_{56}H_{68}N_{10}O_4Si$: C 69.11, H 7.04, N 14.39%, found: C 69.24, H 7.34, N 14.03%.

General preparation procedure for compounds 1–3-QSi. The related axially disubstituted phthalocyanine (compound **1-QSi** (30 mg, 0.376 mmol), compound **2-QSi** (30 mg, 0.339 mmol), or compound **3-QSi** (30 mg, 0.376 mmol)) was dissolved in chloroform (3 mL). Then iodomethane (for compound **1-QSi** (11 mg, 0.753 mmol), for compound **2-QSi** (10 mg, 0.678 mmol), for compound **3-QSi** (9 mg, 0.617 mmol)) was added to the reaction content. The mixture was stirred at room temperature for 48 hours. The solid was filtered off, washed several times with chloroform, and dried in a vacuum.

Compound 1-QSi. Yield 20 mg (48%), mp >250 °C. FT-IR ν (cm^{-1}): 3071 (C–H aromatic), 2970–2944 (C–H aliphatic), 1365–1203 (C–N). ^{1}H NMR (500 MHz; DMSO-d_6): δ (ppm) 7.90–7.82 (m, 8H, Ar–H), 7.63–7.55 (m, 8H, Ar–H), 3.60 (bs, 14H, 4 N–C**H**$_2$–CH_2–CH_2–CH_3, 2 NCH_3), 1.76–1.68 (m, 16H, 4 N–CH_2–C**H**$_2$–C**H**$_2$–CH_3), 1.40–1.33 (m, 12H, 4 N–CH_2–CH_2–CH_2–C**H**$_3$). UV–vis (DMSO): λ_{max} nm ($\log \varepsilon$) 339 (5.17), 619 (5.02), 677 (5.27). MS *m*/*z* calcd for $[M]^+$ 1080.95 found 370.790 $[M + Na + 3H]^{3+}$, 1098.322 $[M + H_2O]^+$. Anal. calcd for $C_{50}H_{58}I_2N_{10}Si$: C 55.56, H 5.41, N 12.96%, found: C 55.68, H 5.70, N 12.58%.

Compound 2-QSi. Yield 27 mg (68%), mp >250 °C. FT-IR ν (cm^{-1}): 3055 (C–H aromatic), 2960–2920 (C–H aliphatic), 1332–1119 (C–N), 1069 (C–O–C). ^{1}H NMR (500 MHz; DMSO-d_6): δ (ppm) 8.99–8.93 (m, 8H, Ar–H), 8.52–8.41 (m, 8H, Ar–H), 3.56 (bs, 14H, 4 N–C**H**$_2$–CH_2–CH_2–CH_3, 2 N–CH_3), 1.72–1.61 (m, 8H, 4 N–CH_2–C**H**$_2$–CH_2–CH_3), 1.39–1.34 (m, 8H, 4 N–CH_2–CH_2–C**H**$_2$–CH_3), 0.93–0.86 (m, 12H, C**H**$_3$), −1.65 to −1.68 (m, 4H, 2 N–C**H**$_2$–CH_2–O–Si), −2.58 to −2.61 (m, 4H, 2 N–CH_2–C**H**$_2$–O–Si). UV–vis (DMSO): λ_{max} nm ($\log \varepsilon$) 334 (5.19), 617 (5.01), 670 (5.07). MS *m*/*z* calcd for $[M]^+$ 1169.06 found 801.787 $[M - 2C_4H_9 - 2I]^+$, 1019.596 $[M - C_4H_9 - I + 2H_2O]^+$, 1169.825 $[M]^+$, 1226.733 $[M + Na + 2H_2O - 2H]^+$, 1284.636 $[M + 2Na + 3H_2O - 2H]^+$. Anal. calcd for $C_{54}H_{66}I_2N_{10}O_2Si$: C 55.48, H 5.69, N 11.98%, found: C 55.64, H 6.03, N 11.57%.

Compound 3-QSi. Yield 29 mg (74%), mp >250 °C. FT-IR ν (cm^{-1}): 3063 (C–H aromatic), 2957–2926 (C–H aliphatic), 1161–1334 (C–N), 1075 (C–O–C). ^{1}H NMR (500 MHz; DMSO-d_6): δ (ppm) 8.30 (bs, 8H, Ar–H), 7.60–7.53 (m, 8H, Ar–H), 3.52–3.49 (m, 14H, 4 N–C**H**$_2$–CH_2–CH_2–CH_3, 2 NCH_3), 1.43–1.34 (m, 16H, 4 N–CH_2–C**H**$_2$–C**H**$_2$–CH_3), 1.17–1.12 (m, 4H, 2 N–C**H**$_2$–CH_2–O–CH_2–CH_2–O–Si), 1.07–1.01 (m, 12H, 4 N–CH_2–CH_2–CH_2–C**H**$_3$), 0.82–0.77 (m, 8H, 2 N–CH_2–C**H**$_2$–O–C**H**$_2$–CH_2–O–Si), 0.64 (bs, 4H, 2 N–CH_2–CH_2–O–CH_2–C**H**$_2$–O–Si). UV–vis (DMSO): λ_{max} nm ($\log \varepsilon$) 332 (5.00), 610 (4.83), 669 (4.72). MS *m*/*z* calcd for $[M]^+$ 1257.17 found 557.856 $[M - CH_3 - I]^{2+}$, 1669.429 $[M + 2DHB + 3Na + 2H_2O]^+$. Anal. calcd for $C_{58}H_{74}I_2N_{10}O_4Si$: C 55.41, H 5.93, N 11.14%, found: C 55.59, H 6.33, N 10.75%.

Biological studies

DNA cleavage experiments. The DNA cleavage activity of quaternized phthalocyanines (**1–3-QSi**) was monitored using agarose gel electrophoresis.[58] Supercoiled pBR322 plasmid DNA (100 μg, Sc) was utilized without irradiation. Supercoiled pBR322 plasmid DNA was treated with compounds **1–3-QSi** ranging from 50 to 200 μM in DMSO and DDW. All samples were incubated at 37 °C for 24 hours in PCR tubes. Then, the mixtures were loaded on 1% agarose gel with ethidium bromide staining in TAE buffer (Tris acetic acid–EDTA). Electrophoresis was carried out at 90 V for 70 min and the results were visualized by applying the BioRad Gel Doc XR system and analyzed using the Image Lab version 4.0.1 software program.

DNA binding experiments using gel electrophoresis. Quaternized phthalocyanines (**1–3-QSi**) were dissolved in DMSO to obtain 200 μM solutions. Agarose gel electrophoresis experiments were performed to support the interaction of the studied compounds with CT-DNA.[32,35] In this study, a series of samples included one of the studied compounds (50 μM) and different concentrations of CT-DNA (0.25–2 mg mL^{-1} in DDW). The total volume of each mixture was adjusted to a final volume of 25 μL with DDW in PCR tubes and incubated at 37 °C for 1 h. Then, the mixtures were loaded with the buffer on 1% agarose gel with ethidium bromide staining in TAE. The electrophoresis was carried out at 90 V for 1 h. The results were visualized using the BioRad Gel Doc XR system.[62] The study for CT-DNA was designed using AL-DNA instead of CT-DNA. The interaction of samples with AL-DNA was examined by applying gel electrophoresis.

DNA binding measurements using UV–vis spectrophotometry. A PerkinElmer Lambda 25 UV–vis spectrophotometer at Erciyes University Nanotechnology Research Center was used. The absorption intensities of 50 μM quaternized phthalocyanines (**1–3-QSi**) were measured in the absence and presence of different concentrations of CT-DNA (2–0.25 mg mL^{-1}) in aqueous media after incubation for 1 hour at 37 °C. The mixtures were diluted by the addition of 5 mM Tris–HCl/50 mM NaCl buffer (pH 7.2).[32] The K_b values were calculated by applying the method extensively described in ref. 83.

Topoisomerase inhibition. The human DNA topoisomerase I and *E. coli* topoisomerase assays were performed as described previously with minor modifications.[62]The human topoisomerase I (Topo I) inhibition activity of quaternized phthalocyanines (**1–3-QSi**) was investigated by measuring the relaxation of supercoiled pBR322 plasmid DNA (100 μg) in the absence/presence of the studied compounds (200–50 μM) in buffer (10× TGS) and dilution buffer in the kit. The mixtures were incubated at 37 °C for 1 h. Then, 4 μL of 5× loading buffer solution consisting of 4.5% SDS, 0.25% bromophenol blue, and 45%

glycerol was added. Electrophoresis was carried out in 1% agarose gel in 1× TAE at 90 V for 90 min[84]

The *E. coli* topoisomerase I (Topo I) inhibition activity of compounds **1–3-QSi** was investigated by measuring the relaxation of supercoiled pBR322 plasmid DNA (100 μg) in the presence of the compounds (200–50 μM) in only one buffer of the kit. The mixtures were adjusted to a final volume of 20 μL with DDW and incubated at 37 °C for 1 h. Then, 4 μL of 5× loading buffer solution consisting of 4.5% SDS, 0.25% bromophenol blue, and 45% glycerol was added. Electrophoresis was carried out in 1% agarose gel in 1× TAE at 90 V for 90 min. Irinotecan (2 mg mL^{-1}) was used as a positive control in two enzyme studies.

Cell culture. The human colorectal cell line (DLD-1) was obtained from the American Type Culture Collection CCL-221™, ATCC, (USA). Cells were cultured in DMEM supplemented with 10%FBS, 1% L-glutamine, and 1% penicillin–streptomycin. Cells were incubated at 5% CO_2 in a 37 °C humidified incubator.[75,76] Cells were cultured in 75 cm^2 flasks.

MTT assay. For the MTT assay, the tested cells were seeded as 1×10^4 cells per well in 96 well plates. After 24 h, different volumes of the studied compounds were added to the cells to obtain 3.125, 6.25, 12.5, 25, 50, and 100 μM. DMSO (30%) was used as a negative control and non-treated cells were utilized as the control group. For the dark group, a 96-well plate was incubated in 5% CO_2 in a humidified incubator at 37 °C for 24 h. For the white light irradiation (light exposure) group, the 96-well plate was incubated for 1 hour under normal conditions and then the plates were moved for 1 hour under white light irradiation. After 1 hour, the plates were removed for the normal incubation conditions. The white lamp was 3000 lx and the distance between the plate surface and the light source was 4 cm. After incubation, MTT solution (0.5 mg mL^{-1} final concentration) was added to the wells and the formazan crystals were observed after 3 h.[85] The well contents were aspirated and 100 μL DMSO was added to solve formazan crystals. The data were recorded between 560 and 750 nm using an ELISA reader (Glomax, Promega, USA). Then, the half-maximal inhibitory concentration (IC_{50}) was calculated from the obtained optical density (OD) values.[86,87]

Apoptosis assay. For the apoptosis assay, 1×10^5 cells were seeded on 6-well culture plates. After 24 h, compounds **1–3-QSi** were added to the cells. DMSO was used as negative control and non-treated cells were utilized as the control group. The light exposure group was not tested for this assay. Only the darkness group (normal incubated plates) was analyzed. After 24 h of incubation, the cells were harvested with Trypsin-EDTA and centrifuged. The cell pellet was resuspended with 100 μL dPBS and then 100 μL MUSE Annexin V kit reagent was added. After 20 min, the cells were analyzed using a MUSE Cell Analyzer (Millipore, USA).[88]

Conclusions

This study reports the successful synthesis and characterization of two new ligands and six new silicon phthalocyanines. Compounds **1–3-QSi** exhibited different DNA binding behaviours that depended on the DNA nature (pBR322 plasmid DNA, CT-DNA, and AL-DNA). They displayed a moderate binding propensity to pBR322 plasmid DNA. However, compound **2-QSi** displayed the highest interaction with CT-DNA compared with compounds **1-QSi** and **3-QSi**. Additionally, compounds **1–3-QSİ** interacted with the CT-DNA in intercalation mode. Although compounds **1-QSi** and **2-QSi** strongly bound to the AL-DNA, compound **3-QSi** did not interact with AL-DNA. Therefore, the potential of compound **3-QSi** for use as a pesticide can be studied in the future. All the compounds inhibited the human topoisomerase I enzyme at all the studied concentrations. Compound **1-QSi** demonstrated a low inhibition effect whereas compounds **2-QSi** and **3-QSi** exhibited normal inhibition activities against *E. coli* topoisomerase I. In addition, the *in vitro* cytotoxic and apoptotic effects of the newly synthesized compounds **1–3-QSi** were examined on the DLD-1 cell line using MTT and Annexin V assays, respectively. The studied phthalocyanines had phototoxic effects on the cell *in vitro*. However, there was no statistical difference between the dark group and the white lamp irradiation group under the applied conditions. IC_{50} values were obtained between 10.61 and 14.16 μM in this study. As the chain length in the molecules increased, their cytotoxic properties improved. To conclude, these compounds can be used as multidisciplinary biological agents for various environmental and medical applications after further investigations.

Conflicts of interest

There are no conflicts to declare.

Acknowledgements

This work was supported financially by the Scientific and Technological Research Council of Turkey (TUBITAK; 220Z023).

Notes and references

1 C. C. Leznoff and A. B. P. Lever, *Phthalocyanines: Properties and Applications*, VCH, New York, 1989, 1993 and 1996, vol. 1–4.
2 J. A. Elvidge and R. P. Linstead, *J. Chem. Soc.*, 1955, 3536.
3 Ö. Bekaroğlu, *Appl. Organomet. Chem.*, 1996, **10**, 605.
4 R. P. Linstead and A. R. Lowe, *J. Chem. Soc.*, 1934, **214**, 1022.
5 A. Beduoğlu, A. M. Sevim, A. Koca, A. Altındal and Z. A. Bayır, *New J. Chem.*, 2020, **44**, 5201.
6 M. P. Polat, D. Akyüz, H. Y. Yenilmez, A. Koca, A. Altındal and Z. A. Bayir, *Dalton Trans.*, 2019, **48**, 9194.
7 H. P. Karaoğlu, A. Atsay, I. Nar, V. McKee, M. B. Koçak, E. Hamuryudan and A. Gül, *J. Mol. Struct.*, 2019, **1197**, 736.

 This journal is © The Royal Society of Chemistry 2022

8 E. Kumral, H. Y. Yenilmez, S. Albayrak, A. N. Şahin, A. Altındal and Z. A. Bayır, *Dalton Trans.*, 2020, **49**, 9385.
9 Ö. İpsiz, H. Y. Yenilmez, K. Kaya, A. Koca and Z. A. Bayır, *Synth. Met.*, 2016, **217**, 94.
10 Ö. Sağlam, M. Akin, H. P. Karaoğlu, N. Saki and M. B. Koçak, *ChemistrySelect*, 2020, **5**(8), 2522.
11 A. Kalkan, A. Koca and Z. A. Bayir, *Polyhedron*, 2004, **23**, 3155.
12 H. Y. Yenilmez, A. N. Şahin, A. Altındal and Z. A. Bayır, *Synth. Met.*, 2021, **273**, 116690.
13 N. Farajzadeh, Ç. Çelik, G. Y. Atmaca, S. Özdemir, S. Gonca, A. Erdoğmuş and M. B. Koçak, *Dalton Trans.*, 2022, **51**, 478.
14 E. T. Saka, Z. Biyiklioğlu and H. Kantekin, *Turk. J. Chem.*, 2014, **38**, 1166.
15 N. Farajzadeh, S. Özdemir, S. Gonca, G. Y. Atmaca, A. Erdoğmuş, Z. A. Bayır and M. B. Koçak, Photochem. Photobiol., 2021, Early view, DOI:DOI: **10.1111/php.13553**.
16 R. D. Joyner and M. E. Kenney, *Inorg. Chem.*, 1962, **1**, 236.
17 J.-W. Hofman, F. van Zeeland, S. Turker, H. Talsma, S. A. G. Lambrechts, D. V. Sakharov, W. E. Hennink and C. F. van Nostrum, *J. Med. Chem.*, 2007, **50**, 1485.
18 M. D. Maree, N. Kuznetsova and T. Nyokong, *J. Photochem. Photobiol., A*, 2001, **140**, 117.
19 J. Li, Y. Yang, P. Zhang, J. R. Sounik and M. E. Kenney, *Photochem. Photobiol. Sci.*, 2014, **13**, 1690.
20 M. C. Vebber, T. M. Grant, J. L. Brusso and B. H. Lessard, *Langmuir*, 2020, **36**, 2612.
21 K. Sato, K. Ando, S. Okuyama, S. Moriguchi, T. Ogura, S. Totoki, H. Hanaoka, T. Nagaya, R. Kokawa, H. Takakura, M. Nishimura, Y. Hasegawa, P. L. Choyke, M. Ogawa and H. Kobayashi, *ACS Cent. Sci.*, 2018, **4**, 1559.
22 H. Li, T. J. Jensen, F. R. Fronczek and M. G. H. Vicente, *J. Med. Chem.*, 2008, **51**, 502.
23 D. Anderson, A. P. Gorka and M. J. Schnermann, *Nat. Commun.*, 2016, **7**, 13378.
24 Y. Cheng, T. L. Doane, C.-H. Chuang, A. Ziady and C. Burda, *Small*, 2014, **10**, 1799.
25 S. Riahi, S. Eynollahi and M. R. Ganjali, *Chem. Biol. Drug Des.*, 2010, **76**, 425.
26 G. Bischoff and S. Hoffmann, *Curr. Med. Chem.*, 2002, **9**, 321.
27 A. Ali and S. Bhattacharya, *Bioorg. Med. Chem.*, 2014, **22**, 4506.
28 J. Ferlay, I. Soerjomataram, R. Dikshit, R. Eser, C. Mathers, M. Rebelo, D. M. Parkin, D. Forman and F. Bray, *Int. J. Cancer*, 2015, **136**, 359.
29 (*a*) World Health Organization, Cancer, (2018) **https://www.who.int/cancer/en/** (accessed 4 May 2018); (*b*) American Chemical Society, Cancer Facts and Statistics, (2018) **https://www.cancer.org/research/cancer-facts-statistics.html**, (accessed 4 May 2018).
30 S. M. Pradeepa, H. S. B. Naik, B. V. Kumar, K. I. Priyadarsini, A. Barik and S. Jayakumar, *Inorg. Chim. Acta*, 2015, **428**, 138.
31 T. Keleş, B. Barut, Z. Biyiklioglu and A. Özel, *Dyes Pigm.*, 2017, **139**, 575.
32 B. Barut, Ü. Demirbaş, A. Şenocak, A. Özel and H. Kantekin, *Synth. Met.*, 2017, **229**, 22.
33 C. Uslan and B. Ş. Sesalan, *Inorg. Chim. Acta*, 2013, **394**, 353.
34 X.-M. Shen, B.-Y. Zheng, X.-R. Huang, L. Wang and J.-D. Huang, *Dalton Trans.*, 2013, **42**, 10398.
35 H. Baş, B. Barut, Z. Biyiklioglu and A. Özel, *Dyes Pigm.*, 2019, **160**, 136.
36 D. Pietrangeli, A. Rosa, A. Pepe, S. Altieri, S. Bortolussi, I. Postuma, N. Protti, C. Ferrari, L. Cansolino, A. M. Clerici, E. Viola, M. P. Donzello and G. Ricciardi, *Dalton Trans.*, 2015, **44**, 11021.
37 X.-Q. Zhou, L.-B. Meng, Q. Huang, J. Li, K. Zheng, F.-L. Zhang, J.-Y. Liu and J.-P. Xue, *ChemMedChem*, 2015, **10**(2), 304.
38 L. Zhou, E. Chen, W. Jin, Y. Wang, J. Zhou and S. Wei, *Dalton Trans.*, 2016, **45**, 15170.
39 I. Toubia, C. Nguyen, S. Diring, M. Pays, E. Mattana, P. Arnoux, C. Frochot, M. Gary-Bobo, M. Kobeissi and F. Odobel, *Eur. J. Med. Chem.*, 2012, **58**, 12.
40 S. Sharma, F. Yan, V. A. Doronina, H. Escuin-Ordinas, M. D. Ryan and J. D. Brown, *Nucleic Acids Res.*, 2012, **40**(7), 3143.
41 (*a*) J. D. Watson and F. H. C. Crick, *Nature*, 1953, **171**, 737; (*b*) A. K. Williams, S. C. Dasilva, A. Bhatta, B. Rawal, M. Liu and E. A. Korobkova, *Anal. Biochem.*, 2012, **422**(2), 66; (*c*) C. Ozluer and H. E. Satana Kara, *J. Photochem. Photobiol., B*, 2014, **138**, 36; (*d*) R. Gul, A. Badshah, A. Khan, A. Junaid and M. K. Rauf, *Spectrochim. Acta, Part A*, 2014, **117**, 264.
42 S. Maiti, P. Maiti, S. S. Sinha, R. K. Mitra and S. K. Pal, *Int. J. Biol. Macromol.*, 2009, **44**, 133.
43 B. Weiss, S. Amler and R. W. Amler, *Europe PMC*, 2004, **113**(4), 1030, PMID: 15060196.
44 P. Cabras, A. Angioni, V. L. Garau, E. V. Minelli, F. Cabitza and M. Cubeddu, *J. Agric. Food Chem.*, 1997, **45**, 3221.
45 K. Peker, *Bodenkultur*, 2004, **55**(2), 47.
46 J. D. Watson and F. H. C. Crick, *Cold Spring Harbor Symp. Quant. Biol.*, 1953, **18**, 123.
47 Y. Pommier, *Cancer Chemother. Pharmacol.*, 1993, **32**, 103.
48 B. K. Sinha, *Drugs*, 1995, **49**(I), 11.
49 D. C. McFarland, *Gen. Hosp. Psychiatry*, 2019, **60**, 148.
50 A. Wanchai and J. M. Armer, *Complement Ther. Clin. Pract.*, 2020, **38**, 101074.
51 R. Słota and G. Dyrda, *Inorg. Chem.*, 2003, **42**(18), 5743.
52 S. Alvarez, *Chem. – Eur. J.*, 2020, **26**, 4350.
53 R. Diaz-Torres and S. Alvarez, *Dalton Trans.*, 2011, **40**, 10742.
54 G. Y. Atmaca, M. Aksel, B. Keskin, M. D. Bilgin and A. Erdoğmuş, *Dyes Pigm.*, 2021, **184**, 108760.
55 A.-A. Sorescu, R.-M. Ion, A. Nuta, Spectral and photodynamic properties of a silicon (tert-butil) phthalocyanine, *The Scientific Bulletin of Valahia University – Materials and Mechanics – Nr. 9*, 2014, vol. **9**.

56 Ö. Güngör, G. A. Özpınar, M. Durmuş and V. Ahsen, *Dalton Trans.*, 2016, **45**, 7634.
57 (*a*) P. Shi, M. Lin, J. Zhu, Y. Zhang and Q. Jiang, *J. Biochem. Mol. Toxicol.*, 2009, **23**, 295; (*b*) S. Gowda, B. B. Mathew, C. N. Sudhamani and H. S. B. Naik, *Biomed. Biotechnol.*, 2014, **2**, 1.
58 W. Xiao, X. Guan, B. Huang, Q. Ye, T. Zhang, K. Chen, Y. Peng and F. Fu, *Dyes Pigm.*, 2021, **186**, 109013.
59 J. Deng, T. Li, G. Su, Q. Qin, Y. Liu and Y. Gou, *J. Mol. Struct.*, 2018, **1167**, 33.
60 J. J. Champoux, *Annu. Rev. Biochem.*, 2001, **70**, 369.
61 W. Duan, W. Zhenxin and M. J. Cook, *J. Porphyrins Phthalocyanines*, 2009, **13**, 1255.
62 T. Keleş, B. Barut, A. Özel and Z. Biyiklioglu, *Dyes Pigm.*, 2019, **164**, 372.
63 E. Bağda, E. Yabaş and E. Bağda, *Spectrochim. Acta, Part A*, 2017, **172**, 199.
64 B. Barut, Ü. Demirbaş, A. Özel and H. Kantekin, *Int. J. Biol. Macromol.*, 2017, **105**, 499.
65 Ü. Demirbaş, *Turk. J. Chem.*, 2019, **43**, 1646.
66 L. Shuai, S. Wang, L. Zhang, B. Fu and X. Zhou, *Chem. Biodivers.*, 2009, **6**, 827.
67 N. S. Boopathy and K. Kathiresan, *J. Oncol.*, 2010, 214186, 18 pages.
68 G. Gregoriadis, J. Senior and G. Poste, *Targeting of Drugs With Synthetic Systems*, Plenum Press, New York and London Published in cooperation with NATO Scientific Affairs Division, 1985.
69 Q. L. Li, W. X. Gu, H. Gao and Y. W. Yang, *Chem. Commun.*, 2014, **50**, 13201.
70 J. B. Huang, H. Liang, D. Cheng and J. Lu, *Polym. Chem.*, 2016, **7**, 1792.
71 L. Li, H. Tian, J. He, M. Zhang, Z. Li and P. Ni, *J. Mater. Chem. B*, 2020, **8**, 9555.
72 P. M. Schlag, B. H.-J. Senn and S. Gallen, *Recent Results in Cancer Research Chemosensitivity Testing in Oncology*, Springer-Verlag Berlin Heidelberg GmbH, Germany, 2003.
73 A. Kamkaew, S. H. Lim, H. B. Lee, L. V. Kiew, L. Y. Chung and K. Burgess, *Chem. Soc. Rev.*, 2013, **42**, 77.
74 F. A. Schaberle, *Photodiagn. Photodyn. Ther.*, 2018, **23**, 75.
75 B.-Y. Zheng, X.-Q. Yang, Y. Zhao, Q.-F. Zheng, M.-R. Ke, T. Lin, R.-X. Chen, K. K. K. Ho, N. Kumar and J.-D. Huang, *Eur. J. Med. Chem.*, 2018, **155**, 24.
76 B. Aru, A. Günay, E. Şenkuytu, G. Y. Demirel, A. G. Gürek and D. Atilla, *ACS Omega*, 2020, **5**, 25854.
77 J. Wu, Y. Wu and B. B. Yang, *Life Sci.*, 2002, **71**, 2161.
78 J. D. Aguirre, A. M. Angeles-Boza, A. Chouai, C. Turro, J.-P. Pellois and K. R. Dunbar, *Dalton Trans.*, 2009, 10806.
79 B. Barut, Z. Biyiklioglu, C. Ö. Yalcin and M. Abudayyak, *Dyes Pigm.*, 2020, **172**, 107719.
80 J. Barge, R. Decre'au, M. Julliard, J.-C. Hubaud, A.-S. Sabatier, J.-J. Grob and P. Verrando, *Exp. Dermatol.*, 2004, **13**, 33.
81 M. E. Rodriguez, P. Zhang, K. Azizuddin, G. B. Delos Santos, S.-m. Chiu, L.-y. Xue, J. C. Berlin, X. Peng, H. Wu, M. Lam, A.-L. Nieminen, M. E. Kenney and N. L. Oleinick, *Photochem. Photobiol.*, 2009, **85**, 1189.
82 J. J. Doyle and J. L. Doyle, *Focus*, 1990, **12**, 13–15.
83 A. Wolfe, G. H. Shimer and T. Meehan, *Biochemistry*, 1987, **26**, 6392.
84 J. G. Deng, T. Li, G. Su, Q.-P. Qin, Y. Liu and Y. Gou, *J. Mol. Struct.*, 2018, **1167**, 33.
85 N. Shivran, M. Tyagi, S. Mula, P. Gupta, B. Saha, B. S. Patro and S. Chattopadhyay, *Eur. J. Med. Chem.*, 2016, **122**, 352–365.
86 M. Abudayyak, E. Güzel and G. Özhan, *Neurochem. Int.*, 2017, **108**, 7–14.
87 M. Patel, N. Pandey, J. Timaniya, P. Parikh, A. Chauhan, N. Jain and K. Patel, *RSC Adv.*, 2021, **11**(44), 27627.
88 S. Akkoç, *ChemistrySelect*, 2019, **4**(17), 4938.

This journal is © The Royal Society of Chemistry 2022